# Energy transfer and photoluminescence properties of lanthanide-containing polyoxotitanate cages coordinated by salicylate ligands

Ning Li,[a,b] Gomathy Sandhya Subramanian,[b] Peter D. Matthews,[a,c] James Xiao,[d] Vijila Chellappan,[b] Timothy E. Rosser,[a] Erwin Reisner,[a] He-Kuan Luo,[b]* and Dominic S. Wright[a]*

a. Department of Chemistry, University of Cambridge, Lensfield Road, CB2 1EW, UK.

b. Institute of Materials Research and Engineering, Agency for Science, Technology and Research, 2 Fusionopolis Way, 08-03, Innovis, Singapore, 138634.

c. School of Chemical and Physical Sciences, Lennard-Jones Building, Keele University, Keele, Staffordshire, ST5 5BG, UK.

d. Cavendish Laboratory, University of Cambridge, J. J. Thomson Avenue, CB3 0HE, UK.

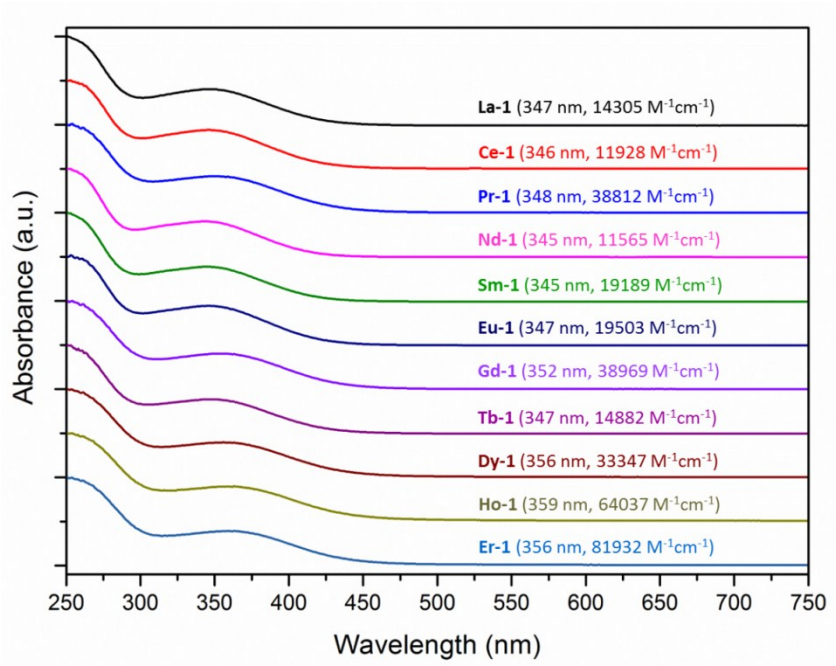


**Fig. S1.** UV-Vis absorbance spectra of the **Ln-1** compounds in anhydrous chloroform. The peak position and extinction coefficients for the *ca.* 350 nm band differ slightly, depending on the choice of $Ln^{3+}$ ion.

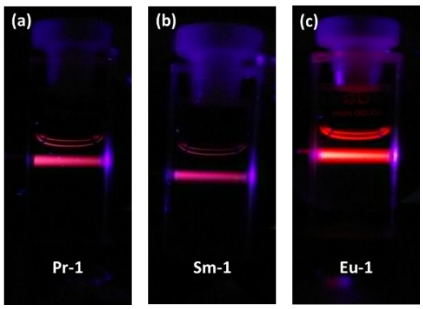


**Fig. S2.** Digital pictures of the photoluminescence of (a) **Pr-1**, (b) **Sm-1** and (c) **Eu-1** in anhydrous *n*-pentane

solution upon excitation by a 405 nm laser beam.

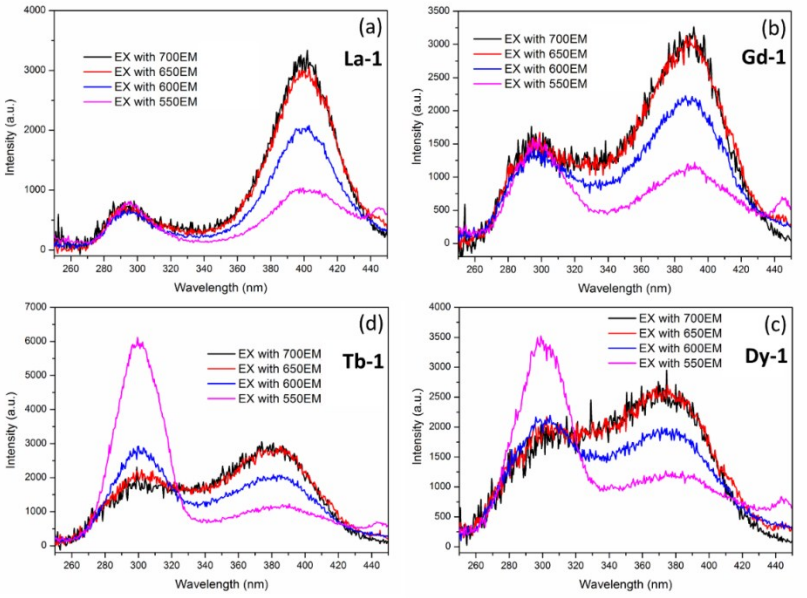


**Fig. S3.** The excitation spectra upon monitoring emission signals across the 700 - 550 nm range in 50 nm steps for (a) **La-1**, (b) **Gd-1**, (c) **Tb-1** and (d) **Dy-1** in anhydrous *n*-pentane solution.

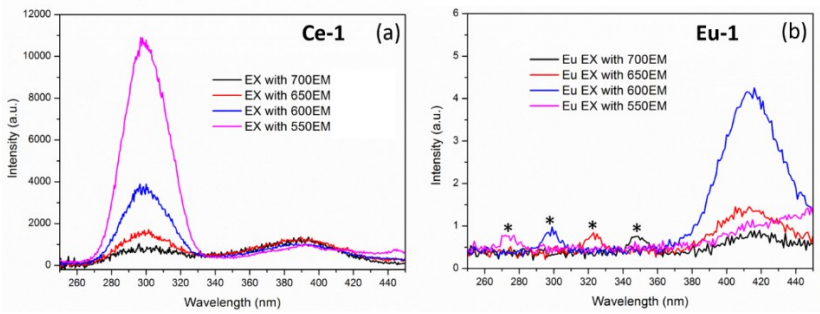


**Fig. S4.** The excitation spectra upon monitoring emission signals across the 700 - 550 nm range in 50 nm steps for (a) **Ce-1** and (b) **Eu-1** in anhydrous *n*-pentane. The peaks labeled with '*' in (b) is not from **Eu-1**, as their positions are exactly half of the monitored emission wavelengths. The difference between the excitation spectra of **Ce-1** and those shown in Fig. S3 could be due to the relatively lower energy required for the *d-f* transitions of $Ce^{3+}$ ions, although further investigations are required to reveal the detailed mechanisms behind this. In contrast, the unique shape of the **Eu-1** excitation spectra is due to the fact that emission signals from the $Eu^{3+}$ ion can be clearly observed. Therefore, the excitation spectra are dominated by the $Eu^{3+}$-centered emission signals, instead of the shifting of the monitored emission wavelengths.

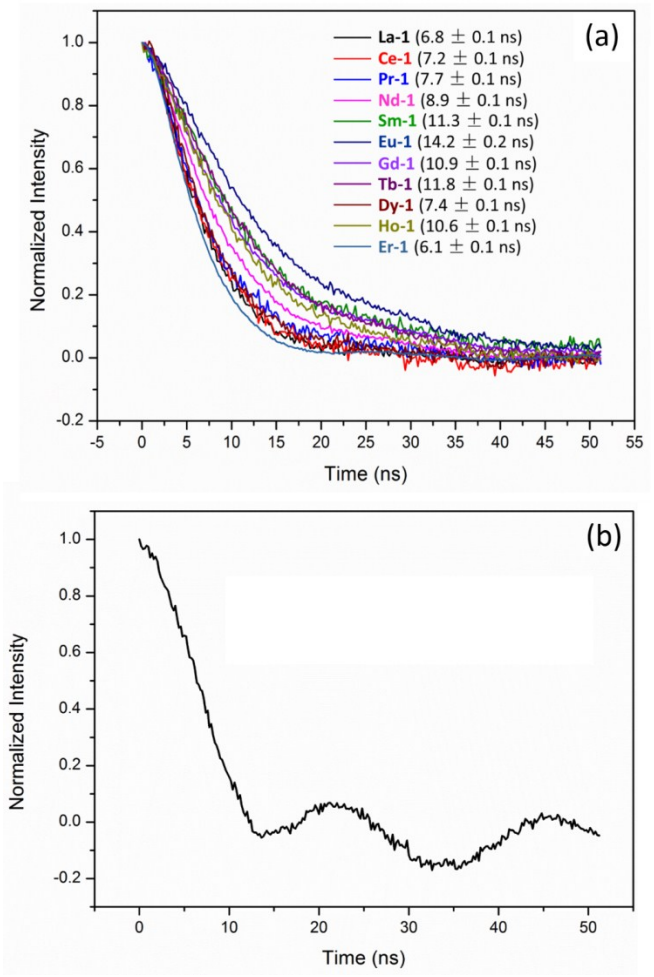


**Fig. S5.** (a) Decaying profile of the emission signal at 525 nm for respective **Ln-1** cage; calculated lifetimes using single exponential curve fitting are also shown; (b) decaying profile representing the response of the equipment employed.

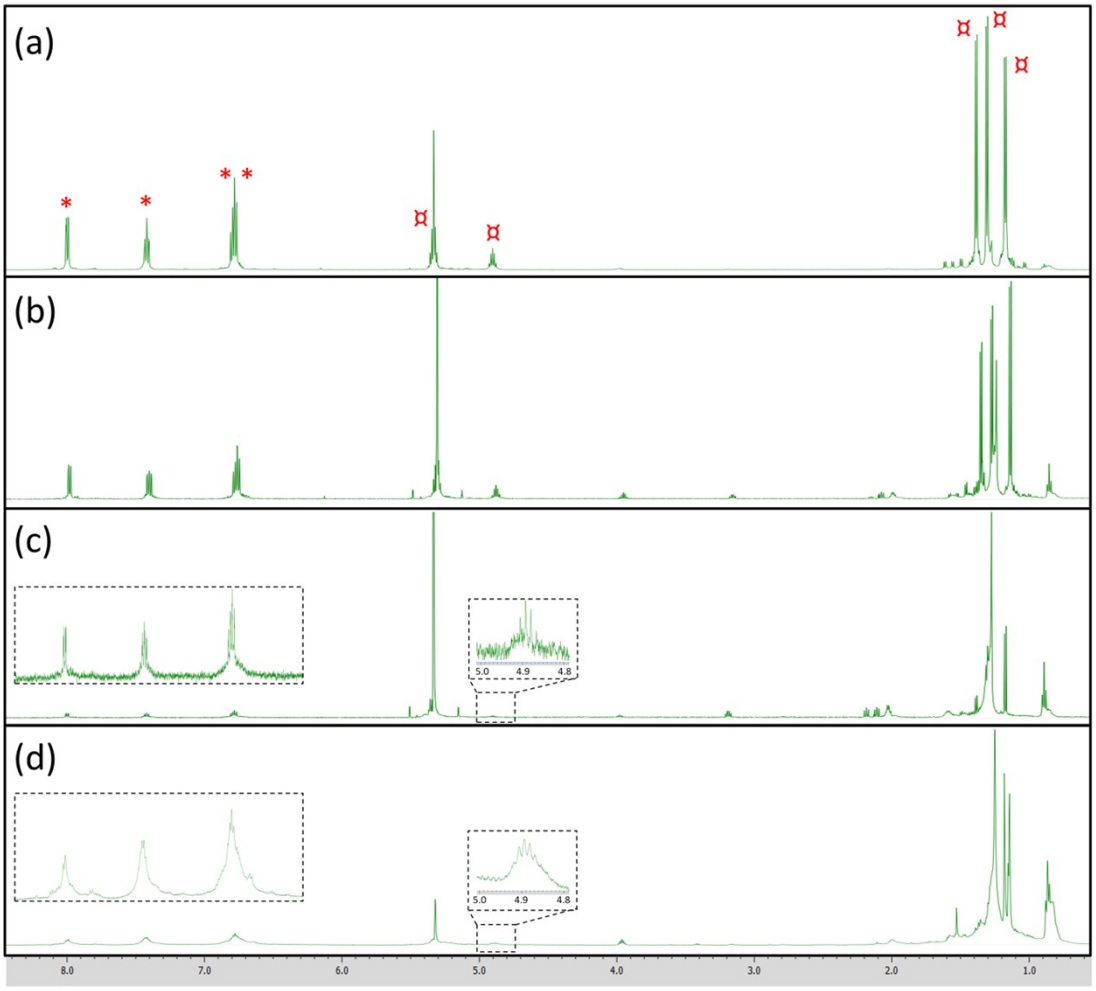


**Fig. S6.** $^{1}$H NMR spectra of **La-1** at room temperature with the sample prepared by: (a) dissolving 5.2 mg **La-1** in 0.7 mL anhydrous $CD_2Cl_2$; (b) dissolving one crystal block of **La-1** (around 0.5 mg) in 0.7 mL anhydrous $CD_2Cl_2$. The resultant solution is of similar colour with that used for photoluminescence study; (c) further diluted by 5 times from the sample in (b); (d) *in vacuo* removing the *n*-pentane solvent from the prepared **La-1** sample for photoluminescence study, and re-dissolving the solid residue in 0.7 mL anhydrous $CD_2Cl_2$. It is clearly seen that both the $^{1}$H signals from the salicylate aromatic ring (denoted by '*') and that from the isopropoxide groups (denoted by '¤'; the signal at around 5.3 ppm overlaps with the residual signal from $CD_2Cl_2$) are all well resolved, indicating that majority of the **La-1** cages retain their molecular structure in dilute solution.

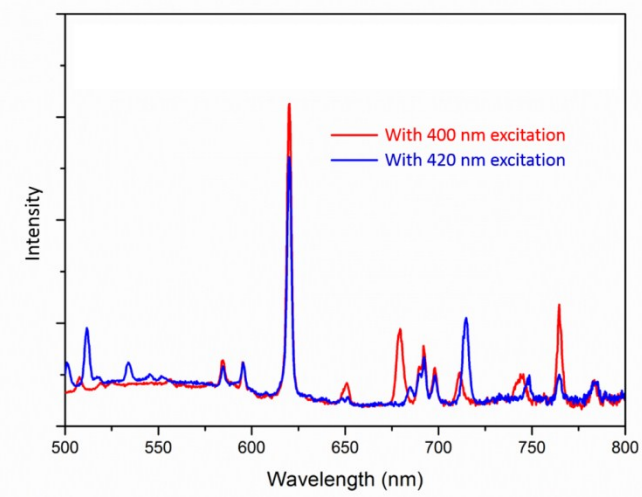


**Fig. S7.** Emission spectra of solid-state **Eu-1** sample with excitation at 400 nm (red trace) and 420 nm (blue trace).

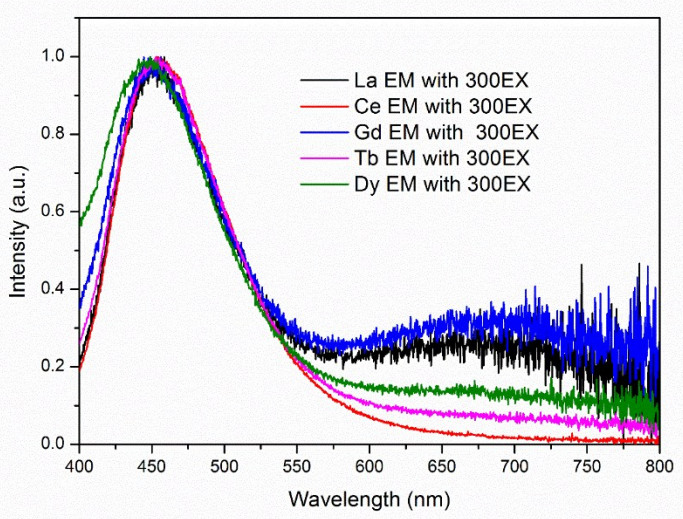


**Fig. S8.** Comparison of the normalized steady-state emission spectra for **La-1**, **Ce-1**, **Gd-1**, **Tb-1** and **Dy-1**. The normalization was based on the main emission band at *ca.* 450 nm.

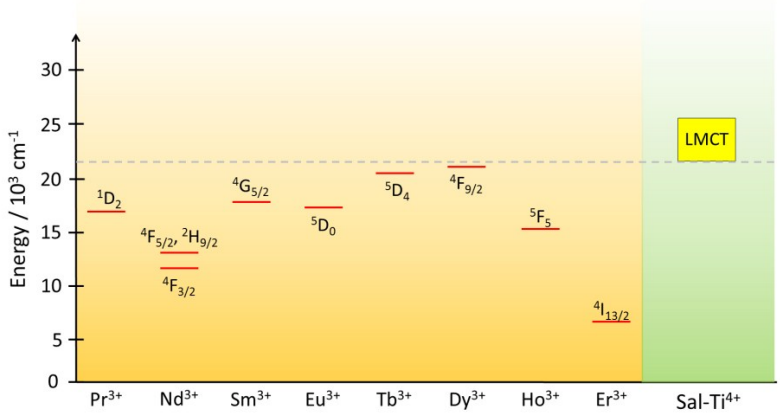


**Fig. S9.** Energy diagram of the proposed LMCT state and the emissive state of respective $Ln^{3+}$ ions.